

LA-UR- 10-05379

*Approved for public release;
distribution is unlimited.*

Title: High Resolution Neutron Imaging of Water in the Polymer Electrolyte Membrane

Author(s):
Dusan Spernjak
Partha P. Mukherjee
Rangachary Mukundan
John Davey
Daniel S. Hussey
David Jacobson
Rodney L. Borup

Submitted to: Gordon Research Conference



Los Alamos National Laboratory, an affirmative action/equal opportunity employer, is operated by the University of California for the U.S. Department of Energy under contract W-7405-ENG-36. By acceptance of this article, the publisher recognizes that the U.S. Government retains a nonexclusive, royalty-free license to publish or reproduce the published form of this contribution, or to allow others to do so, for U.S. Government purposes. Los Alamos National Laboratory requests that the publisher identify this article as work performed under the auspices of the U.S. Department of Energy. Los Alamos National Laboratory strongly supports academic freedom and a researcher's right to publish; as an institution, however, the Laboratory does not endorse the viewpoint of a publication or guarantee its technical correctness.

High Resolution Neutron Imaging of Water in the Polymer Electrolyte Membrane

Dusan Spernjak, Partha P. Mukherjee, Rangachary Mukundan,
Jacob S. Spendelow, John Davey, Joseph Fairweather, and Rodney L. Borup

To achieve a deeper understanding of water transport and performance issues associated with water management, we have conducted *in situ* water examinations to help understand the effects of components and operation. High Frequency Resistance (HFR), AC Impedance and neutron radiography were used to measure water content in operating fuel cells under various operating conditions. Variables examined include: sub-freezing conditions, inlet relative humidities, cell temperature, current density and response transients, different flowfield orientations and different component materials (membranes, GDLs and MEAs).

Quantification of the water within the membrane was made by neutron radiography after equilibration to different humidified gases, during fuel cell operation and in hydrogen pump mode. The water content was evaluated in bare Nafion[®] membranes as well as in MEAs operated in both fuel cell and H₂ pump mode. These *in situ* imaging results allow measurement of the water content and gradients in the PEFC membrane and relate the membrane water transport characteristics to the fuel cell operation and performance under disparate materials and operational combinations.

Flow geometry makes a large impact on MEA water content. Higher membrane water with counter flow was measured compared with co-flow for sub-saturated inlet RH's. This correlates to lower HFR and higher performance compared with co-flow. Higher anode stoichiometry helps remove water which accumulates in the anode channels and GDL material. Cell orientation was measured to affect both the water content and cell performance. While membrane water content was measured to be similar regardless of orientation, cells with the cathode on top show flooding and loss of performance compared with similarly operated cells with the anode on top.

Transient fuel cell current measurements show a large degree of hysteresis in terms of membrane hydration as measured by HFR. Current step transients from 0.01 A cm⁻² to 0.68 A cm⁻² consistently show PEM wetting occurring within 5 to 20 sec. Whereas the PEM drying response to the reverse step transient of 0.68 A cm⁻² to 0.01 A cm⁻², takes several minutes. The observed faster wetting response is due to reaction water being produced in the cathode and back diffusing into the membrane. The slower PEM drying is due to the water slowly being removed out of the wetted GDLs. This rate of removal of water and hence the PEM hydration level was found to be influenced strongly by the PTFE loadings in the GDL substrate and Microporous layer (MPL). The drying of the membrane is influenced by both the anode and cathode GDL PTFE loadings. Lower PTFE loading in the anode GDL leads to better membrane hydration probably due to the easier incorporation of water from the anode GDL into the membrane. Similarly a lower PTFE loading in the cathode GDL also results in better membrane hydration probably due to the better water retention properties (less hydrophobic) of this GDL.

Fuel cells operated isothermal at sub-freezing temperatures show gradual cell performance decay over time and eventually drops to zero. AC impedance analysis indicates that losses are initially due to increasing charge transfer resistance. After time, the rate of decay accelerates rapidly due to mass transport limitations. High frequency resistance also increases over time and is a function of the initial membrane water content. These results indicate that catalyst layer ice formation is influenced strongly by the MEA and is responsible for the long-term degradation of fuel cells

operated at sub-freezing temperatures. Water distribution measurements indicate that ice may be forming mainly in the GDLs at -10 °C but are concentrated in the catalyst layer at -20 °C.

High Resolution Neutron Imaging of Water in the Polymer Electrolyte Membrane

Presented by: **Dusan Spernjak**

August 5, 2010

Los Alamos National Laboratory (LANL)

Dusan Spernjak, Partha P. Mukherjee^a, Rangachary Mukundan,
Jacob S. Spendelow, John Davey, Joseph Fairweather, and Rodney L. Borup

^aPresent Address: Oak Ridge National Laboratory

National Institute of Standards and Technology (NIST)

Daniel S. Hussey, David L. Jacobson, and Muhammad Arif

SGL Carbon

Peter Wilde and Ruediger-Bernd Schweiss

Work from DOE Funded Project 'Water Transport Exploratory Studies'



Outline

- Intro/Motivation
- Neutron Imaging & Detector Development
- Measuring Membrane Water Content via High-Res Neutron Imaging
- Summary



Water Uptake by the Membrane

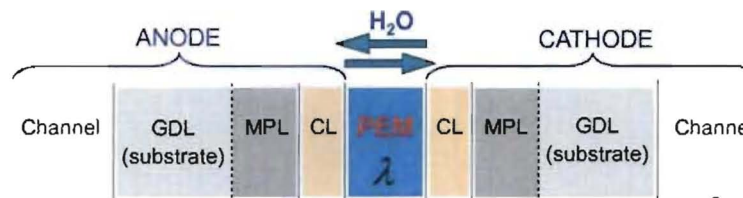
- Membrane conductivity is a function of water content

$$\text{Membrane water content } \lambda = \frac{n_{H_2O}}{n_{SO_3^-}} = \frac{\text{\# of water molecules}}{\text{\# of sulphonic acid sites}}$$

Membrane hydration vs. Excess water removal

→ WATER MANAGEMENT

- Water transport across the membrane (diffusion, electro-osmotic drag) also depends on the hydration state of the membrane

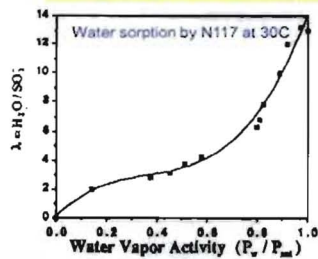


• Los Alamos

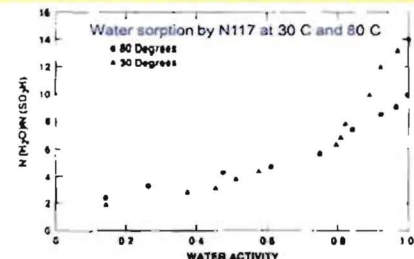
Water Uptake by the Membrane

$$\lambda = \lambda (\text{Relative Humidity})$$

- Historic measurement of water uptake by the membrane:
Ex situ, gravimetric (weight change), free-swelling membrane



T.E. Springer et al, *J. Electrochem. Soc.*, 138, 2334 (1991)



T.A. Zawodzinski et al, *Solid State Ionics*, 60, 199 (1993)

Schroeder's Paradox

$\lambda = 14 @ \text{RH } 100\%$

$\lambda = 22 @ \text{Liquid water}$

- Both 100% RH and liquid water have activity of water = 1.

- Membrane water uptake should be equivalent at these conditions.

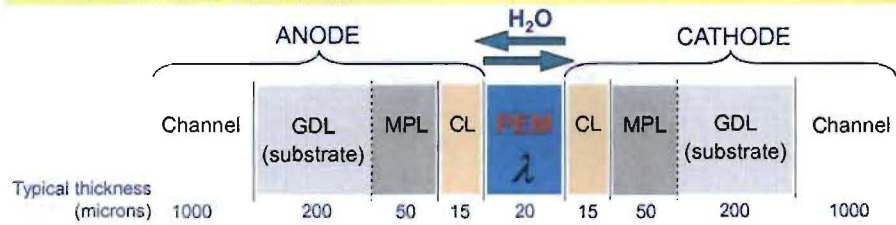
- However, many measurements have been made indicating that this is not true.

Compare to water uptake by the membrane constrained (compressed) by the GDLs and fuel cell hardware

• Los Alamos

Objectives

- Develop understanding of water transport in PEM Fuel Cells
 - Evaluate structural and surface properties of materials affecting water transport, performance, and durability



- NEED to measure water distribution across the fuel cell:
 - Location, Location, Location: Spatially resolved measurement of water content
 - Water-content (saturation) distributions across the thin components of the fuel cell:
 - Gas Diffusion Layer (GDL)
 - Microporous Layer (MPL)
 - Catalyst Layer (CL)
 - Polymer Electrolyte Membrane (PEM)



Approach to Water Exploratory Studies

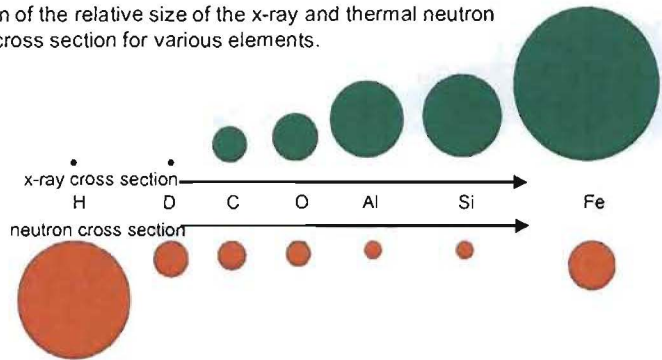
- Experimentally measure water *in situ*
 - Neutron Imaging of water
 - HFR, AC impedance measurements
- Characterization of materials responsible for water transport
- Modeling of water transport within fuel cells
 - Water profile in membranes, catalyst layers, GDLs
- Develop (enable) new components and operating methods



Why Neutron Imaging

Neutrons are an excellent probe for hydrogen in metal since metals can have a much smaller cross section to thermal neutrons than hydrogen does.

Comparison of the relative size of the x-ray and thermal neutron scattering cross section for various elements.

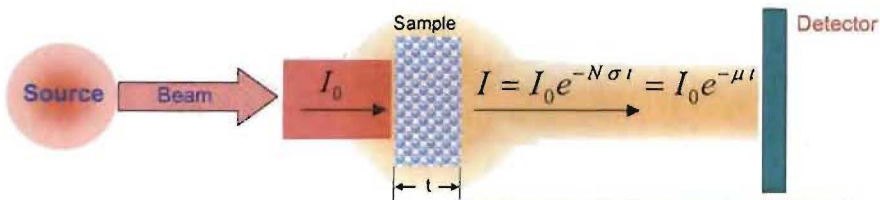


- Heavy elements (more electrons) absorb X-rays better than the light elements.
- Not the case with neutrons (nuclear shell model).



How to get a neutron image?

- **Neutron source** (beam with high enough fluence rate)
Reactor @ NIST NCNR, Thermal Beam tube #2
- **Detector** (to detect/capture neutrons)
(Neutrons are not detected directly → need light or charge)
- Means to convert/resolve the **signal** into **image**



- N – numerical density of sample atoms per cm^3
- I_0 – incident neutrons per second per cm^2
- σ - neutron cross section in $\sim 10^{-24} \text{ cm}^2$
- t - sample thickness
- μ – attenuation coefficient (via calibration)

Beer-Lambert law $I = I_0 e^{-\mu t}$
 I_0 = reference (dry) image
 I = attenuated (wet) image
 μ = attenuation coefficient of water
 t = liquid water thickness



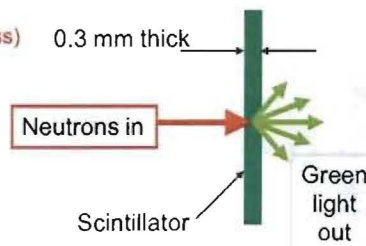
Neutron Detectors I: Scintillators (${}^6\text{Li}$ -doped ZnS)

- Special isotopes that are highly absorbing (${}^6\text{Li}$, ${}^{10}\text{B}$) are used to capture neutrons, resulting in a nuclear reaction that produces charged particles with Mega electron Volt energies:
- ${}^6\text{Li} + \text{n} \rightarrow {}^4\text{He} + {}^3\text{H} + 4.8 \text{ MeV}$
- Converter (traditionally ZnS) stops the particles; energy lost by particles generates a lot of light
- Scintillation light is imaged by a digital camera (CCD or amorphous silicon)
- Thicker scintillator improves the detection efficiency BUT lowers the spatial resolution (which is \sim thickness)**
- NIST scintillator is 0.3 mm thick, yielding a spatial resolution of $0.25 - 0.30 \text{ mm}$



- The spatial resolution of the converter is limited NOT by the nuclear reaction (10 micron range), but by the spread of light in the converter.

How high a resolution is achievable in a neutron detector system ?

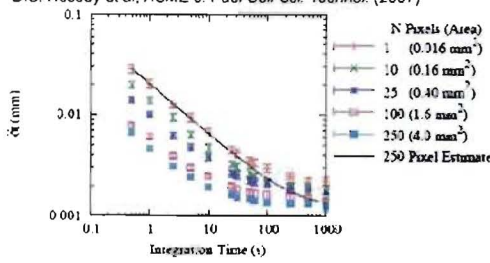


• Los Alamos

Low-Resolution Neutron Detector: amorphous-Si with ZnS

- Spatial Resolution **250-300 μm**
- Pixel Pitch $127 \mu\text{m}$
- Field of View $25 \text{ cm} \times 20 \text{ cm}$
- Frame rate 7.5 Hz max (noisy)
- $10 \mu\text{m}$ water thickness resolution in about 10 seconds
- Automatic dark image removal simplifies processing

Random uncertainty in the water thickness measurement
D.S. Hussey et al, ASME J. Fuel Cell Sci. Technol. (2007)



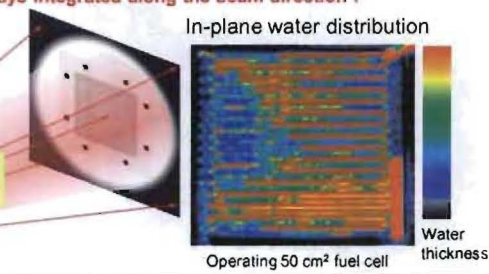
• Los Alamos

Water Distribution and Neutron Imaging

Water content (thickness) is always integrated along the beam direction !

"In-plane water distribution"

- Water content down the channel, land/channel differences
- Neutron beam perpendicular to the membrane plane
- Difficult to distinguish between anode and cathode, or between channel and GDL/MEA
- Allows higher temporal resolution



Low-Resolution Neutron Imaging

Good for:

- Large fuel cells
- Flow field design (channel/land pattern, shape, dimensions)
- Manifold design
- Transients (higher temporal resolution)
- Freeze/Thaw cycling

For fundamental studies & model validation ...

Need to separate water content between ANODE / CATHODE: GDL / MPL / CL / PEM

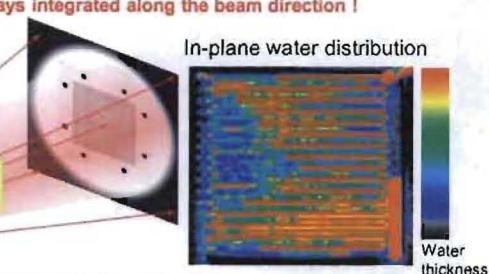
• Los Alamos

Water Distribution and Neutron Imaging

Water content (thickness) is always integrated along the beam direction !

"In-plane water distribution"

- Water content down the channel, land/channel differences
- Neutron beam perpendicular to the membrane plane
- Difficult to distinguish between anode and cathode, or between channel and GDL/MEA
- Allows higher temporal resolution

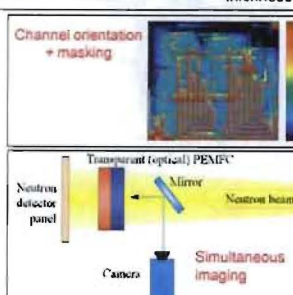


Challenge:

- Separate water content through the cell thickness (beam direction)

Approach:

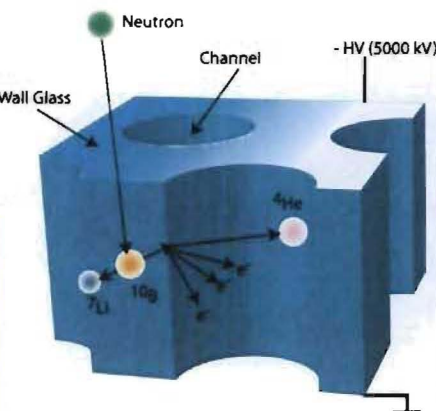
- Cell design (perpendicular or offset anode and cathode channels/lands)
 - + image processing (masking)
- Simultaneous neutron and optical imaging
- High-resolution neutron imaging of the cell cross-section



• Los Alamos

Neutron Detectors II: Micro-Channel Plates (MCP)

- ^{10}B or ^{nat}Gd in wall glass absorbs neutron
- Reaction particles initiate electron avalanche
- Spatial resolution limited by channel separation and range of charged particle
Ultimate resolution $\sim 10 \mu\text{m}$
- Need to resolve the pulses: Charge cloud detected with position-sensitive anode
- High-res detector (anode) development
 - MCP XDL (cross delay line)
Resolution = $25 \mu\text{m}$
 - MCP XS (cross strip)
Resolution = $13 \mu\text{m}$



O.H.W.Siegmund et al, *Nuc. Inst. Meth. Phys. Res. A*, 579 (2007)



Current Neutron detectors: a-Si and MCP

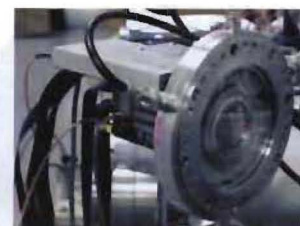
a-Si Panel with ZnS

- 250-300 μm Spatial Resolution
- 127 μm Pixel Pitch
- 25 cm x 20 cm Field of View
- 30 Hz max frame rate
- 1 Hz min frame rate
- 10 μm water thickness resolution in about 10 seconds
- Automatic dark image removal simplifies processing



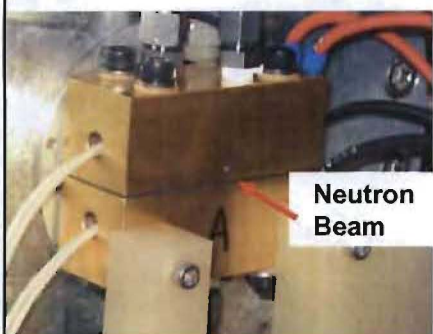
MCP Detector with XDL

- 13 μm Spatial Resolution
- 5 μm Pixel Pitch
- 4 cm diameter Field of View
- ≈ 0.1 Hz max frame rate - Noisy
- 30 μm water thickness resolution per pixel in about 1 h
- Gamma sensitive glass, requires taking dark image



Fuel Cell Design for High-Resolution Neutron Imaging

Previous work, XDL 25 μm detector



Advantages:

- Observe and distinguish between MEA and anode and cathode GDLs and flow fields in x-section
- The high resolution (~25 μm) MCP detector provides the capability of resolving the water content of these thin fuel cell components

Fuel Cell Design Constraints:

- Maximum field of view is 2 cm X 2 cm
- Outermost fuel cell edge in neutron beam path should be no more than 3 cm from detector for good imaging
- The neutron beam should not pass through more than 1 cm of cumulative liquid water
- There should be minimal hydrogen containing compounds in the neutron beam path

Our Cell:

- Active area: 2.25 cm^2 , 1.12 cm X 2.0 cm
- Hardware = gold plated aluminum, gaskets = fiberglass reinforced PTFE
- ~ 1 cm active-area beam path length
- Shallow single serpentine flow field channel (0.6 mm wide X 0.25 mm deep). Realistic pressure drop $\sim 1/3^{\text{rd}}$ that of the 50 cm^2 cell

• Los Alamos

Water Distribution and Neutron Imaging

Water content (thickness) is always integrated along the beam direction !

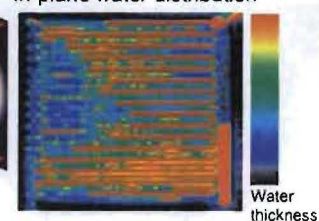
"In-plane water distribution"

- Water content down the channel, land/channel differences
- Neutron beam perpendicular to the membrane plane
- Difficult to distinguish between anode and cathode, or between channel and GDL/MEA
- Allows higher temporal resolution

Circular aperture



In-plane water distribution



Water thickness

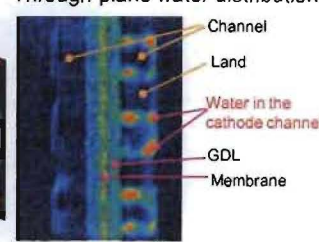
"Through-plane water distribution"

- Water content across the PEMFC sandwich
- Neutron beam parallel to the membrane plane
- Able to distinguish between anode and cathode, or between channel and GDL/MEA
- Need high spatial resolution to resolve the water profile across the GDL/MEA
- Low temporal resolution

Slit aperture

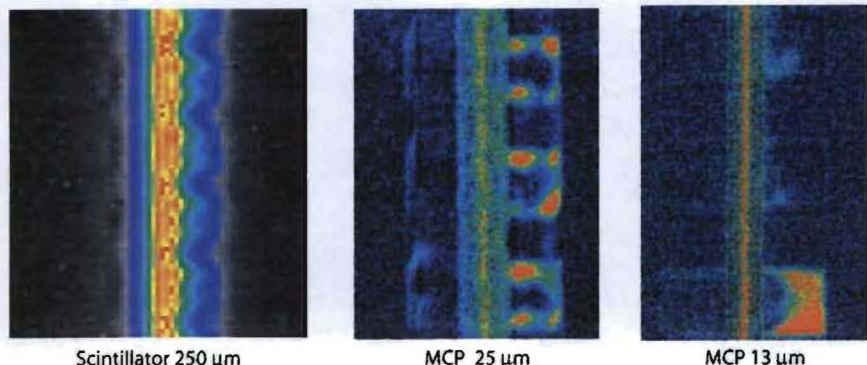


Through-plane water distribution



• Los Alamos

Spatial Resolution of a Neutron Image



- Direct measurement of the GDL water content with 25 μm MCP
- Easily resolve anode from cathode and channel slugs
- 25 μm insufficient to resolve water in auto-competitive membrane
- New 13 μm MCP and slit aperture system greatly improves situation
- But ... there is a systematic uncertainty from the finite resolution

• Los Alamos

Water Profiles for Different Membrane Geometries

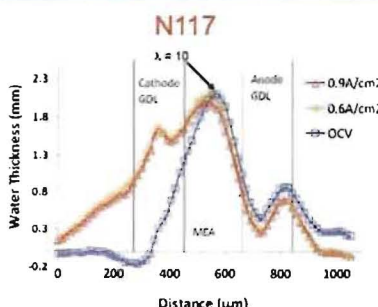


Fig. 4. Water density profile of an operating fuel cell with a Nafion® 117 membrane. $T = 40^\circ\text{C}$, 100% anode/cathode RH, 6mg/cm² Pt, SGL GDL 24 B°C (20% PTFE in Substrate and 10% PTFE in MPL)

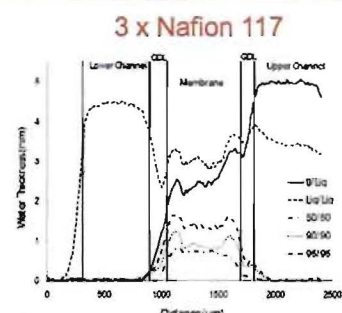


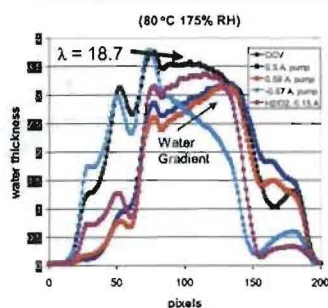
Figure 5. Water distributions for the 3 x Nafion® 117 membrane in the MEA configuration at 0 A/m² or liquid and vapor equilibrium model water vapor concentration (mg/g).

- Interface between membranes is hydrophobic
 - Water peaks in the middle of each Nafion 117 membrane slice
- Interface between membrane and catalyst layer maybe hydrophilic
 - Water peaks near each of the catalyst layers (liquid water in catalyst layer pores)
- XDL I detector: spread function makes it difficult to discern membrane water tests with extremely thick membranes: 3 layers of N117 (hot-pressed) and 40 mil thick membrane

• Los Alamos

Water Profiles for Different Membrane Geometries

40 Mil Nafion Membrane (40 mil ~ 1000 micron)



3 x Nafion 117

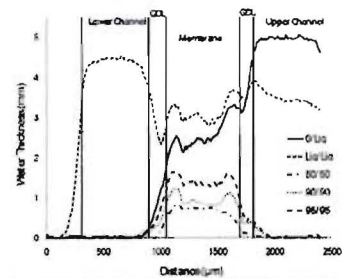


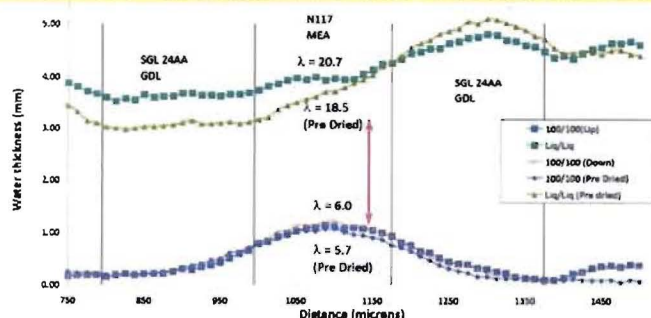
Figure 7: Water absorption for the 3-layer Nafion® 117 membrane in the MEA configuration at 80°C in liquid and vapor equilibrium modes under varying humidification levels.

- Interface between membranes is hydrophobic
 - Water peaks in the middle of each Nafion 117 membrane slice
- Interface between membrane and catalyst layer maybe hydrophilic
 - Water peaks near each of the catalyst layers (liquid water in catalyst layer pores)
- Can clearly distinguish membrane profiles
- Water gradient formed at saturated conditions by H₂ pump
- Previous neutron imaging: qualitative data on water content in the membrane (resolution + spread function) – need accurate in situ measurement of λ

• Los Alamos

Thermal History: In Situ Measurements Verifying Schroeder's Paradox

Drying the membrane at elevated temperature of 108 C ("pre dried") did not show significant effect on water uptake at 100% RH and liquid



Membrane N117, with catalyst layer, and PTFE-free GDL, in nitrogen stream at 80 C
Increase RH from dry to 100% to liquid, and back to 100% and dry
Then, membrane dried at 108 C, and RH cycling repeated

Membrane water content decreases from Liquid to water vapor, thus verifying existence of Schroder's Paradox

- XDL II detector shows much improvement

• Los Alamos

Water Uptake Measurement with the 13 μ m High-Res Detector

GOAL: Measure water uptake by the membrane constrained (compressed) by the GDLs and fuel cell hardware

Nafion® membranes 1100 (equivalent weight)
with different thickness N117, N1110, and N1120

GDL used: SGL24AA by SGL Carbon (no PTFE, no MPL)

Flow field = metal foam with inlet and outlet manifolds cut into the base plate
(even compression, min swelling, faster experiment than with lands/channels)

Three levels of membrane constraint:

(1) Constrained: single GDL on each side

(2) Compressed: double GDL on each side, or
single GDL on each side, but with thin gasket

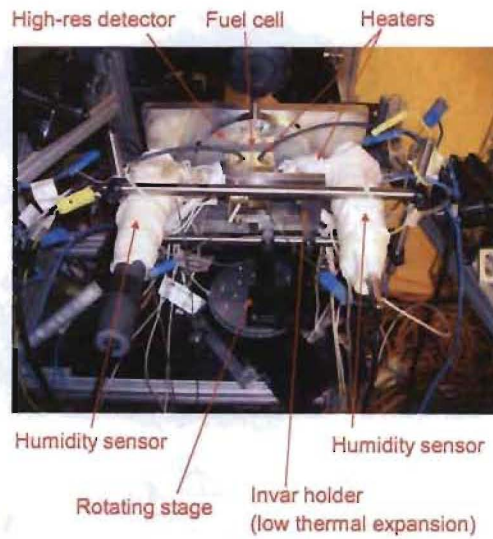
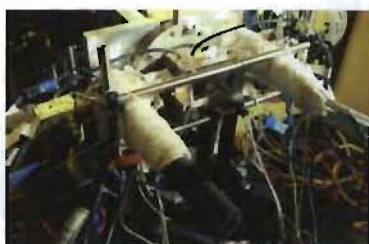
(3) Unconstrained: limited free swelling;
small gap (0.1 to 0.15 mm)
between the membrane and the plate (no GDL)

• Los Alamos

Experimental setup

Recent improvements

- New 13 μ m detector
- Invar holder (min thermal movement)
- Temperature and humidity control:**
- Heat tracing of inlet and outlet lines
- Independent T control of anode and cathode side
- Humidity sensors at the outlets



• Los Alamos

How compressed is the 'compressed' membrane?

Neutron image of the cell cross section

Manifold

No lands and channels (metal foam)

Transmission image intensity profile

Intensity

pixel

Pressure-indicating film
(high color intensity indicates high pressure)
Constrained case: Less than 70 psi
Compressed case: 140 to 200 psi

Compression: constrained vs. compressed

Exposed membrane area

RH cycling – take into account in-plane diffusion over time into the area under gaskets

• Los Alamos

Image Analysis: Beam Hardening

- The effect of beam hardening is that "thick" sections of water appear to be thinner using standard Beer's law
- Can **measure** beam hardening and **accurately** obtain water contents – modeled as a second order polynomial:

$$OD(t) = \ln\left(\frac{I_{\text{wei}} - I_{\text{dark}}}{I_{\text{dry}} - I_{\text{dark}}}\right) = \mu \cdot t + \beta \cdot t^2$$

- However, membrane never fully dries for *in situ* testing; *ex situ* tests show $\lambda_{\text{res}} = 2$
- When normalizing by the dry image, the effect of residual water causes a change in Optical Density vs. water thickness:

$$OD(t + t_{\text{residual}}) = (\mu + 2\beta \cdot t_{\text{residual}}) \cdot t + \beta \cdot t^2$$

- Clear shift in attenuation due to the MEA of a cell in front of the cuvet is shown in bottom figure
- Also checked carbon, aluminum, PTFE, which show no beam hardening effects.

Calibration cuvette placed in front of a fuel cell

Fuel cell

Detector

Calibration cuvette (stepped wedge)

Without a PEMFC

5.5 4.4 3.4 2.4 1.3 0.3 Water depth (mm)

With a PEMFC

• Los Alamos

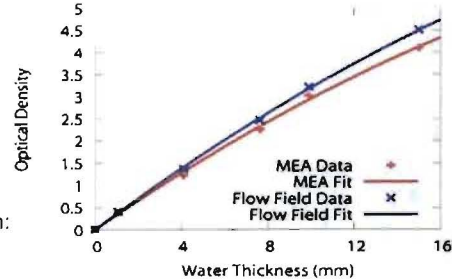
Effect of residual water

- 3 sets of hardware with N117 active widths of 8 mm, 12 mm and 20 mm



- Along with scanning the RH, this enables varying the residual water content
- Measure water attenuation in MEA and Flow Field End Plates: *Clear difference in the linear behavior*
- Residual water was measured by:
 - Obtain OD(t) in flow fields to fix μ & β
 - Fit MEA region allowing only $\lambda_{residual}$ to vary in:

$$OD(t + t_{residual}) = (\mu + 2\beta \cdot t_{residual}) \cdot t + \beta \cdot t^2$$



Effect of residual water

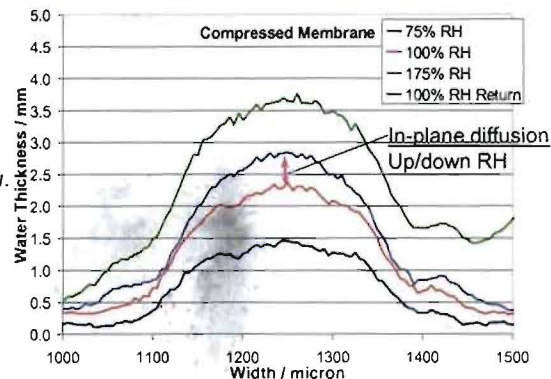
- Need to incorporate residual water into image analysis:
- **How dry is the “dry” image I_o ?**
Need ex-situ measurements to evaluate the reference lambda
- $\lambda_{reference}$ = residual water content in the dry (reference) image
- This value denotes the absolute water content in a membrane in the reference neutron image, and was obtained as the difference between the water content in the membrane at ambient conditions ($\lambda_{ambient} \approx 4$) and the water removed by the pre-imaging drying procedure ($\Delta\lambda \approx 1.7$).
- $\lambda_{reference} = \lambda_{ambient} - \Delta\lambda \approx 2.3$



In situ Measurements of Membrane-Water Equilibrium

NIST's new high resolution detector (13 micron) and N117 (175 micron membrane) to measure water content with varying RH and liquid water reproducible and reversibly *in situ*.

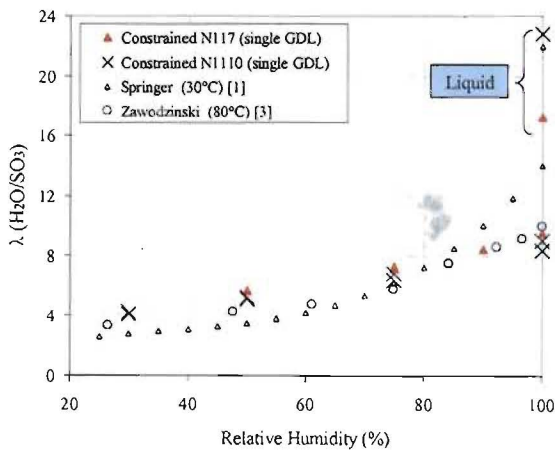
Hysteresis in water content due to in-plane water diffusion



- Measured Membrane water equilibrated with increasing RH, then liquid water, then decreased the humidity
- Membrane water content decreases from Liquid to water vapor, thus verifying existence of Schroder's Paradox

Water Uptake with Constrained Membrane

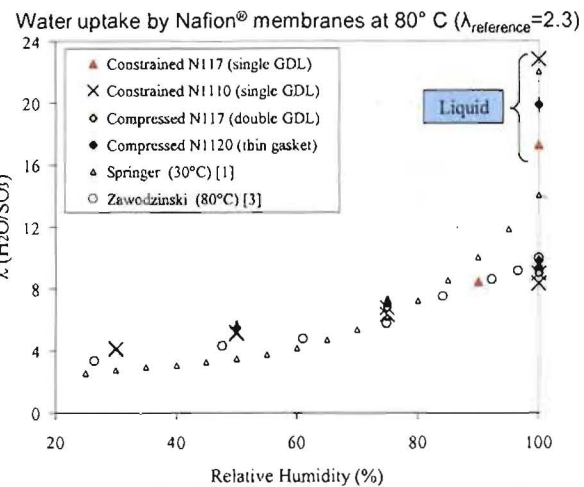
Water uptake by Nafion® membranes at 80° C ($\lambda_{\text{reference}}=2.3$)



Reasonably good agreement with historic data
Slightly higher water content at low RH than previously reported

• Los Alamos

Compression Effect on Water Uptake



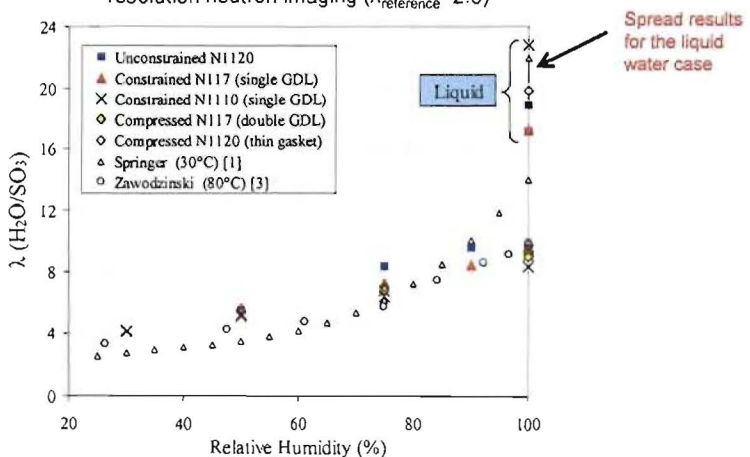
Comparing the constrained and compressed cases, additional membrane compression did not cause significant influence on the water uptake

Possible reason: Membrane expansion in-plane prevented in both cases

• LOS ALAMOS

Lambda Measurements: all 3 cases

Water uptake by Nafion® membranes at 80° C measured by high-resolution neutron imaging ($\lambda_{\text{reference}}=2.3$)



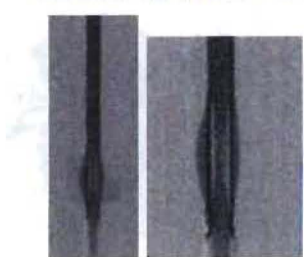
- Unconstrained case shows higher water uptake at elevated RH

• LOS ALAMOS

Unconstrained Membrane

Low lambda at liquid-equilibrated unconstrained membrane:
In-plane swelling (xy plane) causes rippling/ blockage

manifold region shown below



xy plane



Swelling of the membrane included in the analysis.
transmission in the gap region vs. transmission in the bulk membrane

• Los Alamos

GDL: Improved Water Transport Properties

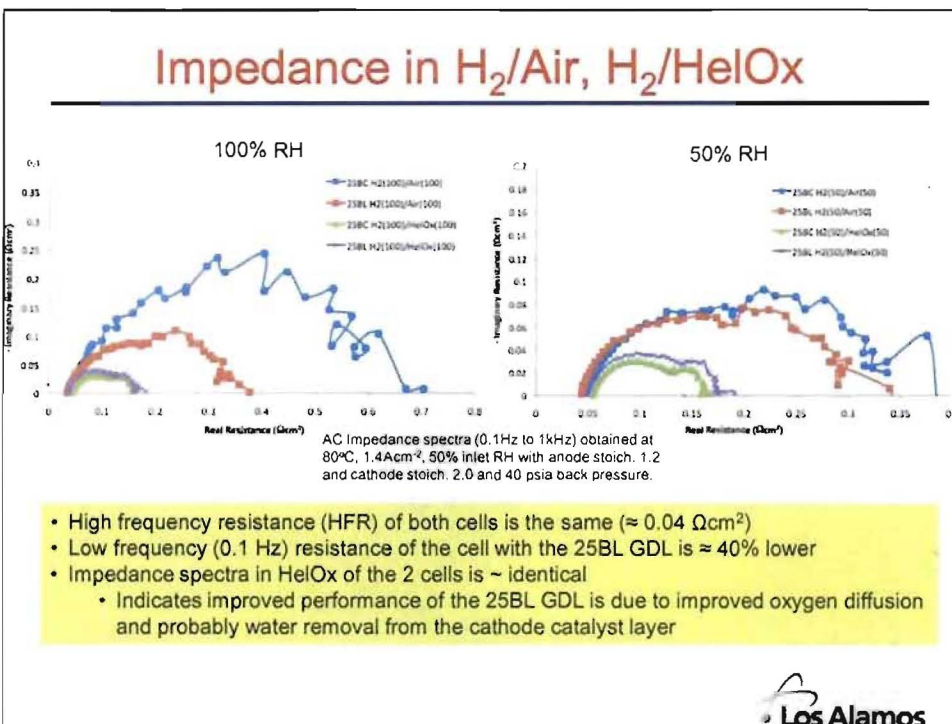
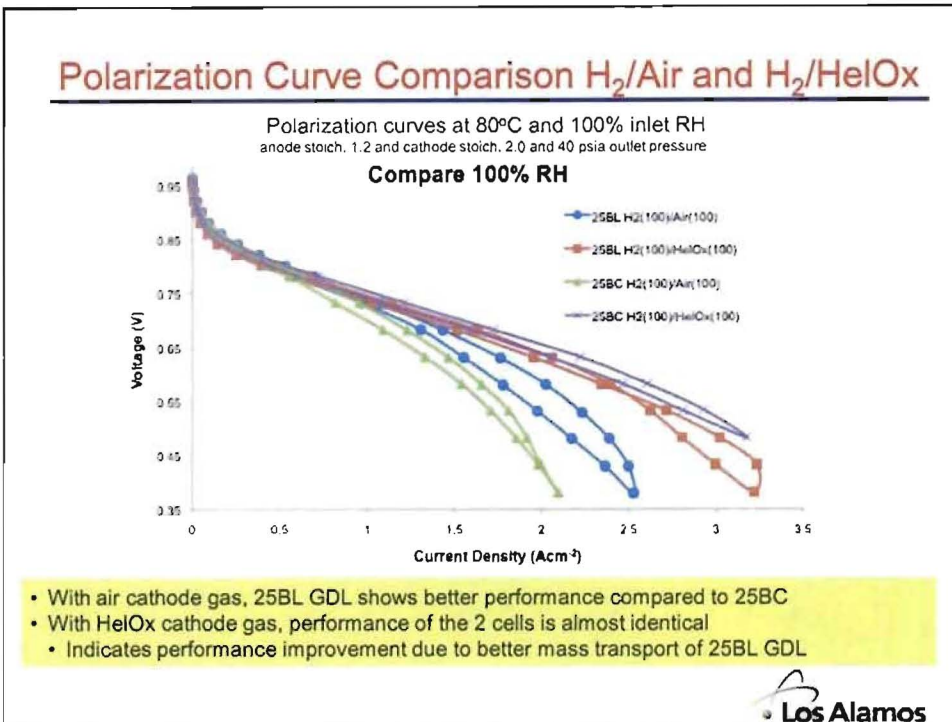
- **GDL Materials**

- Data taken on GDLs varying Teflon loading
- GDL Characterization
- Measured water profiles for various materials
- Measured transport limitations by AC Impedance
- New materials with varying porosity and MPL materials and properties.

Examine novel MPLs with hydrophilic additives (SGL 25BL)

- Added hydrophilic material into MPL (alumosilicate fibers)

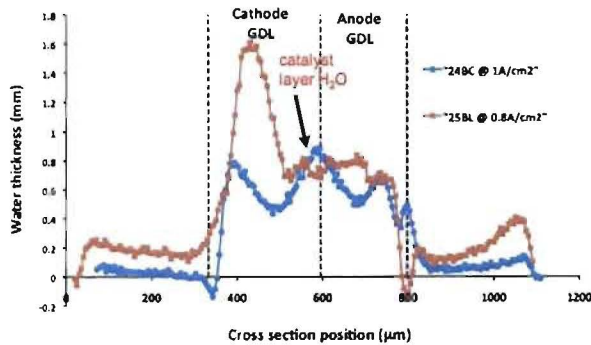
• Los Alamos



GDL Cell comparison, with/without Hydrophilic Cathode MPL Treatment

Neutron Imaging Water Profile Comparison

Whole cell, 80/80°C, 100/100% RH



- Water profile from neutron imaging shows flatter and possibly lower cathode catalyst-layer region water content



Summary

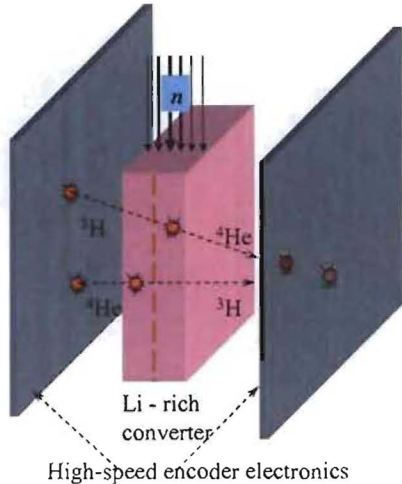
- Membrane water content measurements via neutron imaging
 - In situ RH cycling (increase/decrease)
- Shroeder
- Thermal history effect
- Compression effect
- Agreement with historic data
- Improved experimental setup; detector characterization
- Introduced more accurate image analysis
- High-res capable of resolving water profiles across thicker membranes
- GDL Materials: New materials with modified MPL properties show better water removal characteristics
- Future work – profiles, diffusion, electro-osmotic drag
- Is higher resolution with neutron imaging achievable?



Future Sub-micron Resolution?

- Current technology resolution limit is 10 microns
- Neutron capture by ^6Li results in emission of two charged particles
- The initial energies are well known
- Using Time of Flight difference, the neutron capture event could be localized with an uncertainty of **0.1 micron**
- Proof-of-concept experiment to happen this year?
- A lot of development work yet to be done on fabricating converter
- "Quantum Leap" in detector technology will resolve water profiles in the GDL, MPL, CL and PEM

Also, new beam line (next year?) will add improvement in water sensitivity: cold vs. thermal neutrons (lower integration times)



• Los Alamos

Neutron Detectors III: Sub- μm Resolution

✓ We know:

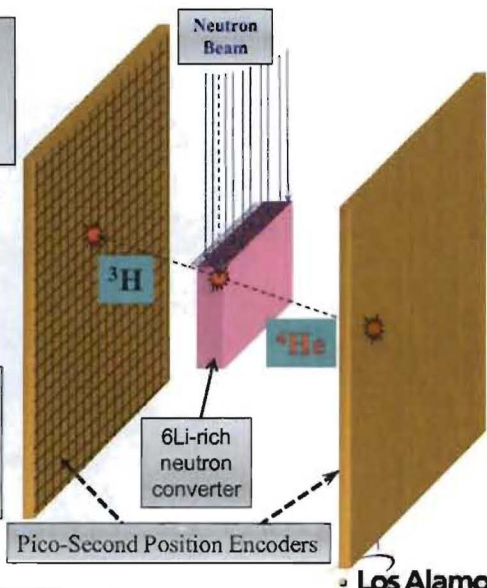
- Initial energy of each particle
- Mass of each particle
- Stopping power

✓ We measure:

- Time of flight
- Point of intersection
- Path/Angle of emissions

✓ Construct image:

- Position (x,y,z)
- Chronology (t)
- Mass density (statistics)

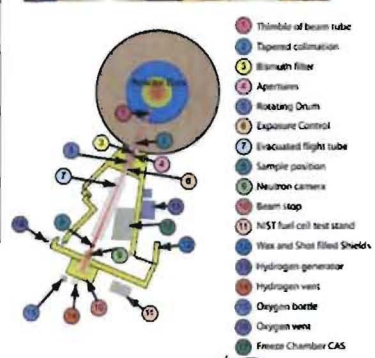


• Los Alamos

The NIST Neutron Imaging Facility at BT2

Current Beam Characteristics

Aperture #	Aperture Dimension	Beam	\approx L/D (x,y)	Fluence Rate
5	15 mm	1	600	6.36E+06
5	15 mm	2	450	1.38E+07
4	10 mm	1	600	4.97E+06
4	10 mm	2	600	6.14E+06
3	3 mm	1	2000	5.23E+05
3	3 mm	2	2000	5.94E+05
2	10 x 1 mm	1	600, 6000	6.54E+05
2	10 x 1 mm	2	600, 6000	8.00E+05
1	1 x 10 mm	1	6000, 600	7.17E+05
1	1 x 10 mm	2	6000, 600	8.13E+05

Los Alamos

NIST Fuel Cell Infrastructure

- Hydrogen Generator, max flow 18.8 slpm
- State of the art Fuel Cell test stand, with graphical User Interface
- Flow control over H₂, Air, N₂, He, O₂:
 - H₂: 0-50, 0-500 and 0-3000 sccm
 - N₂: 0-2000 sccm
 - Air: 0-50, 0-100, 0-500, 0-2000, 0-8000 sccm
 - O₂: 0-500, 0-5000 sccm
 - He: 0-600, 0-6000 sccm
- 1.5 kW boost power supply allowing Voltage control of the cell to a minimum of 0.01V
- Heated Inlet gas lines, Built-in humidification
- 8 T-type thermocouple inputs
- 2 Viasala dew point sensors available
- Interfaced with facility hydrogen safety system
- Freeze Chamber Available to All Users
 - 40 C to +50 C, 1000 kW cooling at -40 C
 - 32" W, 24" H, 18" D sample volume
 - Explosion-proof, and Hydrogen safe
- Zahner IM6eX Electrochemical Workstation available
- All users of the NIST NIF have full access to the Fuel Cell Infrastructure

Fuel Cell Stand



Freeze Chamber Installed inside the Imaging Facility



Los Alamos

NIST: Future Work

- Continue to develop advanced imaging methods for fuel cell research
 - Improve accuracy of water content measurements by implementing new *in situ* measurement of residual water in dry cells
- Continued advancement of imaging technology and capabilities at the facility
 - Improve field of view while maintaining spatial resolution to look at larger fuel cells
 - New large format detectors will be incorporated into the facility to improve acquisition capabilities.
- Add new cold imaging capabilities using new facility to be built for expansion of the NCNR



NIST: Summary of Technical Accomplishments

- High Resolution Neutron Imaging
 - New high resolution neutron imaging system deployed and in use.
 - Measured spatial resolution is 13 μm .
 - High resolution system using scintillator coupled to CCD achieves sub 20 μm spatial resolution
- Search for systematic errors in neutron radiography
 - Determined systematic underestimation of water content
 - Due unaccounted residual water in dry membrane images
 - With beam hardening this results in underestimation of water content
 - Can experimentally measure this effect and obtain true water content of cell
 - Improved humidity control
 - Installed check valve to ensure dry gas at low flow rates and freeze studies
 - Heating all exposed sections of humidified gas lines to eliminate condensation
 - Changed from 0.25" to 0.125" gas lines to improve flow consistency for small scale cells
- Study of water hydration of membranes
 - In collaboration with LANL have studied a range of membrane histories and compositions, anticipate completing the analysis in summer 2010
- Freeze and Purge studies are ongoing
 - Research will benefit from closed-bath chiller with -45 $^{\circ}\text{C}$ to 100 $^{\circ}\text{C}$ range



Differences between Neutron and X-Ray Imaging

- Materials absorb neutrons and x-rays differently.
- X-rays are absorbed by the electron clouds of atoms. High-Z elements (like lead) have more electrons, so they absorb more x-rays. We can say that they have a large "x-ray cross section."
- Unlike x-rays, neutrons are absorbed by atomic nuclei. A nuclide's tendency to absorb neutrons can be understood through the **shell model** of the nucleus.
- Nuclear Shell Model - Just as atoms have electron shells, a nuclide has shells for protons and neutrons (although they are considerably more complicated). Just as some elements (such as chlorine) "want" to grab an electron to fill their shell, some nuclides (like ^3He) "want" to grab a neutron.



Neutrons vs. X-Rays - Summary

- Light elements tend to absorb neutrons far better than x-rays. Hydrogen is among the most significant of these, since it is found in materials like water, plastic, and wax. These materials can be imaged easily with neutrons, but not with x-rays.
- Many common metals like steel, lead, and aluminum are more transparent to neutrons than to x-rays. This can be an advantage, because x-rays are often completely blocked by these materials. Neutrons are absorbed strongly enough for imaging, but not so strongly that all the neutrons are blocked.
- Neutrons are much better for differentiating elements with similar Z. Because of the complexity of the shell model and the strong force, a nuclide's neutron cross section can vary considerably between elements with similar Z, or even between isotopes of the same element.



Publications

- Wang, Yun; Mukherjee, Partha P.; Mishler, Jeff; Mukundan, Rangachary; Borup, Rodney L.. **Cold start of polymer electrolyte fuel cells: Three-stage startup characterization.** *Electrochimica Acta* (2010), 55(8), 2636-2644.
- Wood, David L., III; Rulison, Christopher; Borup, Rodney L.. **Surface Properties of PEMFC Gas Diffusion Layers.** *Journal of the Electrochemical Society* (2010), 157(2), B195-B206.
- Wood, David L.; Chlistunoff, Jerzy; Majewski, Jaroslaw; Borup, Rodney L.. **Nafion Structural Phenomena at Platinum and Carbon Interfaces.** *Journal of the American Chemical Society* (2009), 131(50), 18096-18104.
- Wood, David; Mukundan, Rangachary; Borup, Rodney. **In-plane mass-transport studies of GDL variation using the segmented cell approach.** *ECS Transactions* (2009), 25(1, Proton Exchange Membrane Fuel Cells 9), 1495-1506.
- Davey, John R.; Mukundan, Rangachary; Spendelow, Jacob S.; Mukherjee, Partha; Hussey, Daniel S.; Jacobson, David L.; Arif, Muhammad; Borup, Rodney L.. **Wetting and drying responses of gas diffusion layers and proton exchange membrane to current transients.** *ECS Transactions* (2009), 25(1, Proton Exchange Membrane Fuel Cells 9), 971-983.
- Mukherjee, P. P.; Mukundan, R.; Spendelow, J. S.; Davey, J. R.; Borup, R. L.; Hussey, D. S.; Jacobson, D. L.; Arif, M.. **High resolution neutron imaging of water in the polymer electrolyte fuel cell membrane.** *ECS Transactions* (2009), 25(1, Proton Exchange Membrane Fuel Cells 9), 505-512.
- Mukundan, Rangachary; Lujan, Roger W.; Davey, John R.; Spendelow, Jacob S.; Hussey, Daniel S.; Jacobson, David L.; Arif, Muhammad; Borup, Rodney L.. **Ice formation in PEM fuel cells operated isothermally at sub-freezing temperatures.** *ECS Transactions* (2009), 25(1, Proton Exchange Membrane Fuel Cells 9), 345-355.
- Wang, Yun; Mishler, Jeff; Mukherjee, Partha P.; Mukundan, Rangachary; Borup, Rodney L.. **Pseudo one-dimensional analysis of polymer electrolyte fuel cell cold-start.** *ECS Transactions* (2009), 25(1, Proton Exchange Membrane Fuel Cells 9), 285-294.
- Borup, Rod L.; Mukundan, Rangachary; Davey, John R.; Spendelow, Jacob; Hussey, Daniel S.; Jacobson, David L.; Arif, Muhammad. **In situ PEM fuel cell water measurements.** *ECS Transactions* (2009), 17(1, Fuel Cell Seminar 2008), 263-268.
- Mukundan, R.; Borup, R. L.. **Visualising Liquid Water in PEM Fuel Cells Using Neutron Imaging.** *Fuel Cells* (Weinheim, Germany) (2009), 9(5), 499-505.
- A. Nandy, F. Jiang, S. Ge, C.-Y. Wang, and K. S. Chen, "Effect of cathode pore volume on PEM fuel-cell cold start". *Journal of The Electrochemical Society*, 157 (5) 1-XXXX (2010).
- F. Jiang, Chao-Yang Wang, and K. S. Chen, "Current ramping: a strategy for rapid start-up of PEMFCs from subfreezing environment", *Journal of The Electrochemical Society*, 157 (3) B342-B347(2010).
- M. A. Hickner, K. S. Chen, and S. P. Siegel, "Elucidating Liquid Water Removal in an Operating PEMFC via Neutron Radiography", *Journal of Fuel Science and Technology*, February 2010, Vol. 7, p.011001-1.
- S. Basu, C.-Y. Wang, and K. S. Chen, "Phase change in a polymer electrolyte fuel cell", *Journal of the Electrochemical Society*, 156 (6) B748-B756 (2009).

• Los Alamos

Publications

- Jeffrey Mishler, Yun Wang, Rangachary Mukundan, Rodney Borup, Daniel S. Hussey, David L. Jacobson. **In situ Investigation of Water Distribution in Polymer Electrolyte Fuel Cell Using Neutron Radiography**, submitted to 2010 ECS Transactions
- Rangachary Mukundan, John R. Davey, Joseph D. Fairweather, Dusan Spernjač, Jacob Spendelow, Daniel. S. Hussey, David L. Jacobson, Peter Wilde, Ruediger Schweiss, and Rod L. Borup. **Effect of Hydrophilic Treatment of Microporous Layer on Fuel Cell Performance**, submitted to 2010 ECS Transactions
- Peter O. Olapade, Rangachary Mukundan, John R. Davey, Rodney L. Borup and Jeremy P. Meyers, **Modeling the Dynamic Behavior of Proton-Exchange Membrane Fuel Cell**, submitted to 2010 ECS Transactions
- Partha P. Mukherjee, Eunkyoung Shim, Rangachary Mukundan, and Rodney L. Borup, **Digital Volume Imaging of the PEFC Gas Diffusion Layer**, submitted to 2010 ECS Transactions

• Los Alamos

